

Development of a Pulsed Laser Driver

Group Project: LIDAR in Harsh Weather Conditions

Supervisor: #####

Institution: Carleton University

Author: Abrar Ahmad

Student #: #####

April 11, 2018

Abstract

This project outlines the design and implementation of a high speed laser driver. The driver is a key module in the Light and Range Detection (LIDAR) sensor that is developed in this 4th Year Project. LIDAR sensors are a competitive research and development field and are posed to be significant contributors to the sensor system in the autonomous car industry. This laser driver will allow signal processing algorithms capable of superior object detection to be tested with ease. The laser driver is capable of delivering 10 nanosecond pulses to a laser diode at high repetition rates with a stable high voltage power supply. The optical assembly allows users to drive lasers with wavelengths between 650 nm – 950 nm. The driver is implemented on a 6 cm x 4 cm wide PCB that makes it easily portable and useful as a standalone module in various research studies. An alternative design capable of delivering nanosecond pulses at lower power requirements was also developed in this project. This document provides a detailed record of the design, specifications and implementation for the two laser driver designs, and presents another design that can deliver nanosecond pulses without transistors or MOSFETs.

Acknowledgements

I would like to thank my team members for their support and enthusiasm throughout this project.

It was truly a blessing to work with these people. I would also like to thank our supervisor, #####, for her help and regular meetings to help us keep on track. Finally, this project would not be possible without #####'s assistance and permission to use the lab at odd hours.

Table of Contents

Abstract.....	1
Acknowledgements.....	2
List of Figures	5
1 Introduction	6
1.1 Motivation and Background	7
1.2 Overview	9
1.3 Objectives and Specifications	11
2 Professional Considerations.....	12
2.1 Health and Safety	12
2.1.1 High Voltage Supply	12
2.1.2 Laser Safety	13
2.2 Engineering Professionalism	14
2.3 Project Management	14
3 Theory and Techniques.....	15
3.1 Laser Driver I: Avalanche Transistor	15
3.1.1 Avalanche Driver Schematic	18
3.1.2. Pulse and Parasitic Modelling	19
3.1.3 EMI Shielding.....	23
3.1.4 Avalanche Driver Implementation	23
3.2 Laser Driver II: MOSFET Switching	26
3.2.1 Switching Driver Schematic.....	26
3.2.2 Switching Driver Implementation	29
3.3 Optics Assembly	31
3.4 3D Printing Mechanical Assembly.....	33
4 Achievements.....	34
4.1 Results	34
4.1.1 Avalanche driver	34
4.1.2 Switching driver	39
4.2 Alternative Designs	43
4.2.1 (Successful) Switching laser driver with Alternative Pulse Generator.....	43
4.2.2 Rangefinder with Step Recovery Diode (SRD) and Coaxial cable.....	45

4.3 Discussion.....	46
5 Conclusion.....	48
5.1 Summary	48
5.2 Contributions	49
5.5 Future Work	49
6 References	51

List of Figures

FIG 1: IMPACT OF PULSE WIDTH ON TARGET RESOLUTION [7]	8
FIG 2: SYSTEM OVERVIEW OF LIDAR SYSTEM WITH LASER DRIVER HIGHLIGHTED TO SHOW THE INDIVIDUAL PROJECT [REUSED FROM PRESENTATION]	10
FIG 3: ILLUSTRATION OF AVALANCHE EFFECT [11]	16
FIG 4: BREAKDOWN VOLTAGE DEPENDING ON BASE BIAS CONDITION [12]	17
FIG 5: AVALANCHE LASER DRIVER DESIGN [ADAPTED FROM 15]	18
FIG 6: PASSIVE RC HIGH PASS FILTER [16]	20
FIG 7: FIGURE SHOWING SELF RESONANT FREQUENCY OF CAPACITORS [17]	21
FIG 8: MODELLING PARASITIC COMPONENTS OF CAPACITOR	22
FIG 9: LEFT - TIME DOMAIN MODEL OF AN AVALANCHE PULSE WITH 5NS FWHM. RIGHT – FREQUENCY SPECTRUM OF AVALANCHE PULSE	22
FIG 10: SCHEMATIC FOR AVALANCHE DRIVER CIRCUIT	24
FIG 11: PCB FOR AVALANCHE DRIVER	26
FIG 12: MOSFET BASED LASER DRIVER [ADAPTED FROM 20]	27
FIG 13: PULSE GENERATOR BASED ON PROPAGATION DELAY BETWEEN INPUT AND CLR TERMINAL	28
FIG 14: SCHEMATIC FOR SWITCHING DRIVER CIRCUIT [ADAPTED FROM 20]	29
FIG 15: PCB FOR SWITCHING DRIVER	31
FIG 16: REFLECTANCE GRAPH FOR THE COATING SELECTED FOR THE ASPHERE LENS [23]	32
FIG 17: ILLUSTRATION OF BEAM COLLIMATION WITH ASPHERIC LENS [24]	32
FIG 18: CAD MODEL FOR DRIVER HOLDER	33
FIG 19: TRIGGER AND AVALANCHE PULSE SIGNALS USING 2N2369A TRANSISTOR	35
FIG 20: TRIGGER AND AVALANCHE PULSE SIGNALS USING ZTX415 TRANSISTOR	36
FIG 21: AVALANCHE AND NOISE SIGNALS FROM DRIVER USING ZTX415 TRANSISTOR	37
FIG 22: IMPLEMENTATION OF AVALANCHE DRIVER	38
FIG 23: MEASURED TRACES FROM AVALANCHE DRIVER PCB	39
FIG 24: TEST CIRCUIT FOR MOSFET DRIVER	40
FIG 25: MOSFET SWITCHING WITH MIC4422YN DRIVER. GREEN TRACE: TRIGGER INPUT TO DRIVER. YELLOW TRACE: VOLTAGE AT OUTPUT	41
FIG 26: IMPLEMENTATION OF SWITCHING DRIVER	42
FIG 27: PULSE GENERATOR USING COMPARATORS WITH AN AND GATE [25]	43
FIG 28: LASER DRIVER BASED ON SRD AND COAXIAL CABLE [26]	45

1 Introduction

The goal of this 4th Year Project is to improve current LIDAR (Light Detection and Ranging) systems by improving their performance in harsh weather conditions, such as fog, rain and snow. In this project, a LIDAR sensor will be developed alongside a scanning system to generate a point cloud of the environment with better performance in rain and fog. The point cloud can be used to create a high resolution 3D map of the surroundings. This improved LIDAR will offer a major advantage over traditional LIDAR scanners that are unreliable in harsh environments, and will reduce the complexity of sensor systems in autonomous cars by removing redundant sensors that are employed to compensate for poor performance in harsh weather.

A crucial component of a LIDAR system is the pulsed laser driver. The driver allows a laser diode to transmit optical pulses into the environment. Upon hitting an obstacle, a portion of the light is reflected back and picked up by a receiver module that is part of the LIDAR system. By analyzing the transmitted and received power, we can estimate the distance of an object from the LIDAR. The design and implementation of the laser driver are the focus of this individual portion of the 4th year project.

In this report, the theoretical background for a pulsed laser driver will be provided and the design methodologies will be explored for two driver designs:

- (1) An avalanche transistor driver

(2) A MOSFET switching driver

A section on the will be provided to demonstrate the achievements of this project, and will be followed by an outline of the future work that can be carried out with the laser driver.

1.1 Motivation and Background

LIDAR scanners have become a focal point for major car and robot companies to generate high resolution maps [1-3]. Autonomous cars must operate in all weather conditions and one of the biggest challenges of LIDAR is its ability to do well in these environments [4-6]. LIDAR scanners work by transmitting optical pulses and detecting how long these pulses take to arrive back. This time delay is used to determine if an obstacle is present in the direction that pulse is transmitted in, and provides an estimate for how far the obstacle is. Fog, rain, snow or other atmospheric particulates scatter the LIDAR signal and result in false positives for obstacles. This ultimately reduces civilian safety in vehicle transportation. As LIDAR scanners become prevalent in autonomous aerial and ground vehicles, improving the LIDAR system will improve both the economy (through cheaper LIDAR systems) and civilian safety. An affordable and reliable LIDAR solution equates to a stronger market not only for the LIDAR scanner, but also for related devices that rely on or drive LIDAR solutions [3].

A good LIDAR laser driver will deliver optical pulses with short pulse widths to provide high spatial resolution. The importance of pulse width is demonstrated in the following figure, which is originally intended for a Radar system. The principle in the figure applies equally well to LIDAR

systems when we are interested in mapping objects behind transparent objects, such as windows and windshields. This allows more layers to be obtained and used in the 3D maps that are generated. Such information could be especially useful for decision-making in autonomous vehicles [1].

The figure below shows reflected signals arriving at a receiver from two objects. On the right, the objects are close together and indistinguishable from the received signal, while on the left the objects are more separated. This separation allows them to be distinguished from the received signal.

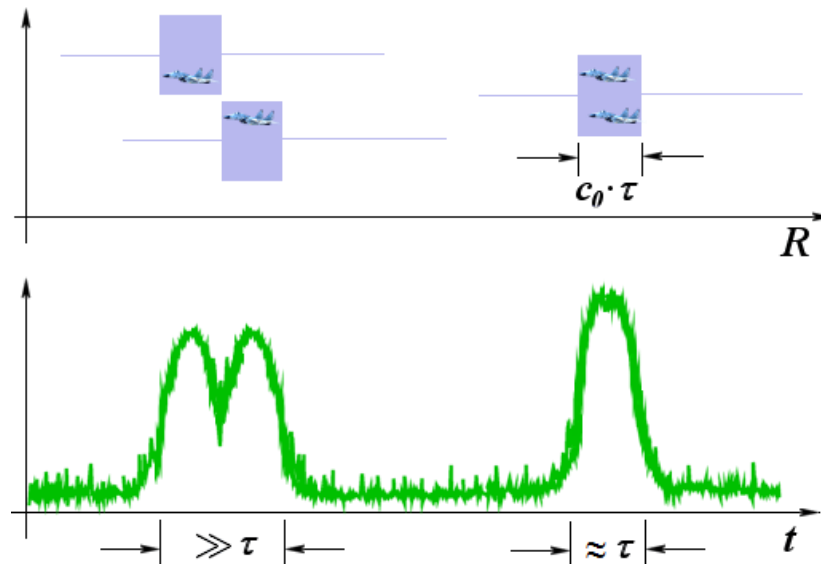


Fig 1: Impact of pulse width on target resolution [7]

The minimum distance that can be resolved by the system is given by the spatial resolution. For the pulses shown in the figure above, the spatial resolution is given by [7]:

$$S_r \geq \frac{c\tau}{2}$$

eq (1)

where c is the speed of pulse in the medium and τ is the pulse width.

When particulates are present in the atmosphere (i.e. during rain and fog), the optical signal will become attenuated due to scattering. The pulses should have a high optical power to compensate for this. By allowing the pulse width to be low, a higher peak power can be used. We therefore want to minimize our pulse width while still allowing the received signal to be sampled with a reasonably fast Analog to Digital Converter (ADC) or sampling technique.

1.2 Overview

The laser driver will be used to make a LIDAR development platform alongside the receiver module. This will allow the driver to be developed in a modular fashion while the other team members develop the scanning and signal processing systems. A block diagram showing the overall project is shown in the figure below.

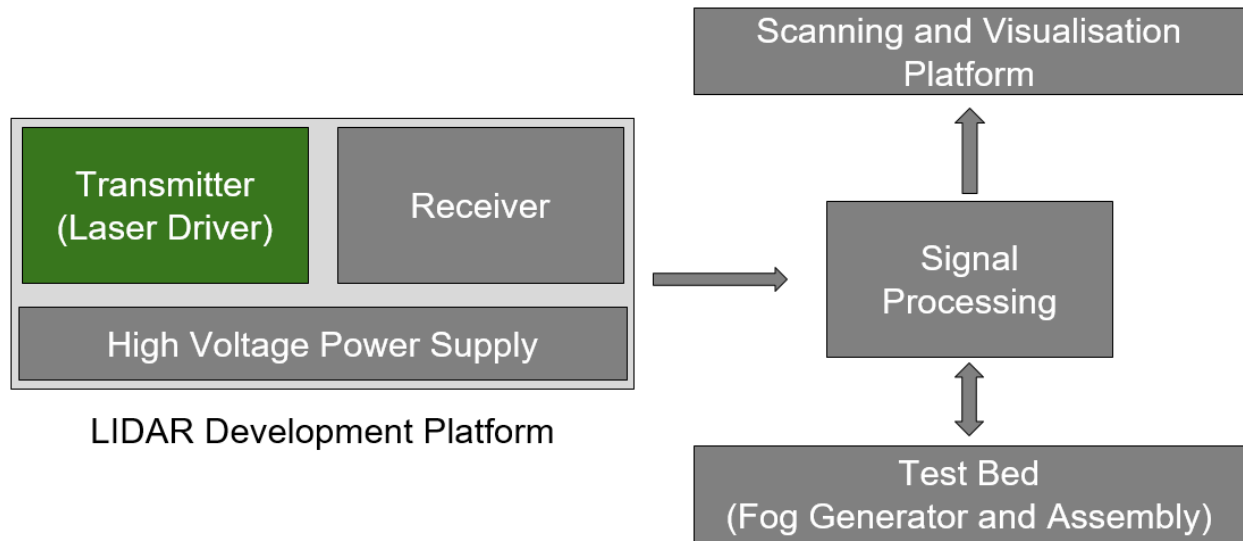


Fig 2: System overview of LIDAR system with laser driver highlighted to show the individual project [Reused from presentation]

As shown in the diagram, the transmitter can be developed independently and tested with a receiver module in 2 ways:

1. An off-the-shelf (e.g. Thorlabs PDA015A) receiver. The receiver should have a sufficiently large bandwidth to allow the received pulses to be recorded, since the pulses have short rise and fall times. This is discussed in more detail in section 3.1.2.
2. Developed by another team member (David Lister).

Once the transmitter and receiver modules (which both utilize high voltage power supplies, as shown in the diagram above) are completed, the development platform can be mounted onto a modified version of the scanning system. The signal processing techniques are developed independently using an off-the-shelf LIDAR system (SF02 Laser Rangefinder by Lightware) and

they will be carried over to the development platform to complete the system integration. The LIDAR system's performance can be verified in the test bed.

1.3 Objectives and Specifications

Due to the modularized nature of the project, each module in figure 2 is required to satisfy certain criteria so that the system integration can be accomplished successfully. These criteria were determined in team meetings to ensure that each module can be used as a black box that provides certain capabilities. The following list outlines the specifications for the laser driver:

1. The laser driver should deliver pulses with pulse widths between 1 and 100 nanoseconds.
A very narrow pulse would make it difficult to sample the optical pulses and would increase the bandwidth requirement of the optical receiver. Meanwhile, a very long pulse width would decrease the spatial resolution, which according to eq (1) is 15 meters with a 100 nanosecond pulse. The aim in this project is to deliver 10 nanosecond pulses, which can be measured with the oscilloscope available for prototyping (Rohde & Schwartz – RTM 2034).
2. The pulses should be transmitted on the rising edge of a 0 – 5 V square pulse trigger. The driver should accept the trigger input using an SMA connector.
3. The driver should provide an output waveform of the pulse transmitted to the laser diode through an SMA connector.

4. The laser driver should require no more than 500 V to operate. This is important because high voltages are required to bias the components in the laser driver. This is discussed in section 3.

2 Professional Considerations

This section outlines the safety considerations in this project and the guidelines for practicing professional engineering. A section on project management is included to show how the deliverables were organized to ensure the project moved smoothly.

2.1 Health and Safety

The laser driver requires a high voltage supply to operate and works with a laser diode. The risks and steps taken to mitigate the risks associated with the power supply and laser diode are given below.

2.1.1 High Voltage Supply

The high voltage power supply for the laser driver operates from a low input voltage (up to 10 volts). The power supply charges a capacitor to a large voltage and it is not capable of delivering continuous power at high voltages. However, the electrical shock from contact with the output terminals can be strong and caution is advised. In order to prevent these shocks, two steps were taken:

- 1) A sufficiently small output capacitor was used in the power supply design to ensure that the energy stored in the capacitor was not very high. This allowed the capacitor to discharge within 10 seconds after the power supply was disconnected and bring the voltage down to safe levels. A $27\ \mu\text{C}$ capacitor was used to ensure that the energy discharged through accidental contact would be small.
- 2) The high voltage supply was always kept on a separate breadboard and isolated from the laser driver circuit using long connector cables.

2.1.2 Laser Safety

The laser driver was prototyped with 7 mW laser diode from Thorlabs (L650P007), and this is classified as a class 3B laser product [8]. Class 3B lasers are hazardous to the eye and can cause retinal burns. However, the laser diode is below 50 mW and the risk is mitigated if the exposure is from a few feet away [9]. In order to prevent any accidents, the following precautions were taken:

1. The laser driver was mainly prototyped with a light emitting diode (LED) and the use of the laser diode was kept to a minimum.
2. The laser diode was operated near any mirrors or reflective surfaces, in order to prevent exposure from reflected light.
3. The laser diode was not used when others were in the lab environment, unless they were team members and were told that the laser is being operated.

2.2 Engineering Professionalism

Engineering is regulated profession and it is regulated by Professional Engineers Ontario (PEO) in Ontario. PEO ensures that only qualified individuals are licensed to practice Engineering by enforcing standards and disciplining those who go against these, or those who act irresponsibly [10]. As this is an Engineering project, care was taken to abide by safety guidelines (especially those mentioned in section 2.1) and conduct ourselves professionally. There were many moments throughout the project where modules had to be redesigned and the requirements had to be reestablished. These changes could affect multiple team members if the specifications of a module were affected. However, each team member conducted themselves in a professional manner and listened to what the others had to say. There was no need to enforce additional discipline throughout the duration of this project. Our team met at odd hours in the evenings and over the weekends to ensure that all roles were moving along as expected, especially since this is a team project.

2.3 Project Management

The deliverables were outlined by the team early in the term and the deadlines were made to give room for error and learning. This was done to ensure that there were no surprises with promising and not delivering. The deliverables were laid out and were assigned to whoever felt most comfortable working on a particular task, or was willing to be challenged. This turned out to be the perfect approach because we were all highly motivated by this project.

The major deadline to work around was the Chinese new year in February (lasting around 2 weeks). The team noted this early in the semester and designed their Printed Circuit Boards (PCBs) before February 15th. This ensured that there was ample time for testing hardware.

In order to manage my individual project, I kept a regular log of the work I had done weekly. Since I did not have previous experience with PCB layout and design, I decided that I would need more than one design for the laser driver. The purpose of this was to minimize the chance of failure, in case one laser driver was faulty (especially during the PCB layout stage).

3 Theory and Techniques

This section provides the theoretical framework and the implementation strategies for the laser driver. Two designs were prepared for the laser driver and the principles behind these are provided in the following subsections. A section on the optics and the mechanical assembly for the laser driver is also included.

3.1 Laser Driver I: Avalanche Transistor

The first design of the laser driver utilized the avalanche effect in an npn transistor to deliver short (pulse width), high power pulses. Avalanche breakdown in a pn junction takes place when a strong electric field is present across the junction due to a large potential difference. Under this potential difference, the electric field is able to accelerate electrons/holes to large kinetic

energies. These electrons/holes can promote valence electrons/holes in the material to the conduction band and still retain enough energy to contribute to the electric current. The new electrons/holes that become part of the conduction band are accelerated by the electric field and cause further impact ionizations. This rapidly gives rise to a multiplication effect and ultimately results in a large current [11]. A depiction of avalanche multiplication is given in the figure below, which shows a single hole (h) giving rise to multiple electrons (e_1, e_2, e_3) and holes (h_1, h_2, h_3).

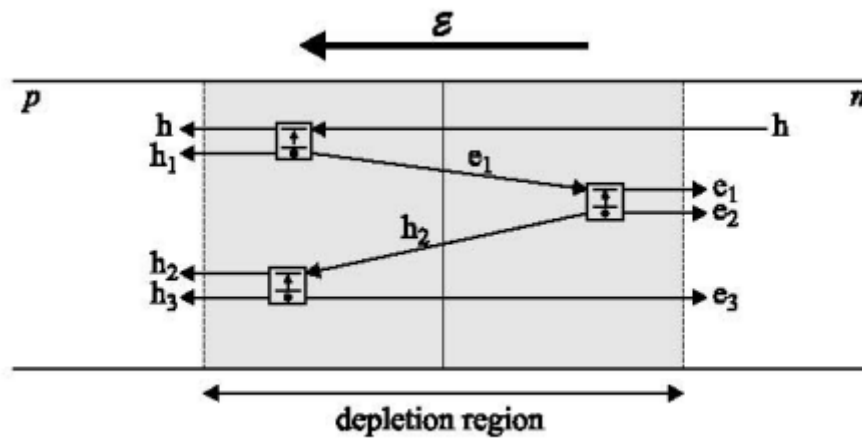


Fig 3: Illustration of avalanche effect [11]

The avalanche effect can be used in an npn transistor by biasing the collector-emitter (CE) junction to a high voltage. The actual voltage required to achieve avalanching is dependent on the device. Depending on the bias of the base junction, the CE junction will break down and avalanching will occur beyond a voltage that is usually given as a threshold voltage [4]. The CE breakdown voltage, V_{BR} is shown in the following figure under different bias conditions for the base.

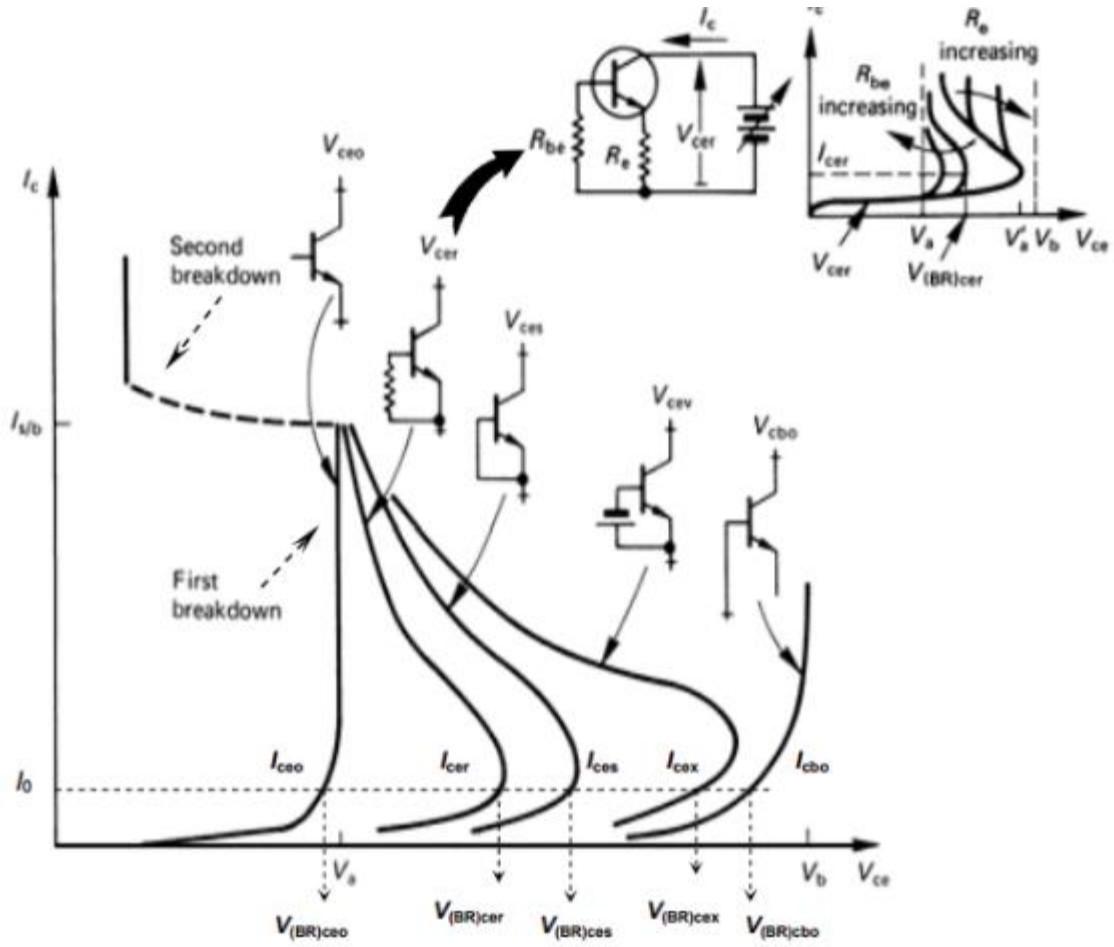


Fig 4: Breakdown voltage depending on base bias condition [12]

The avalanche driver was prototyped with two transistors: the 2N2369A and ZTX415. The datasheets report the minimum breakdown voltages for these transistors as $V_{(BR)CEO} = 15\text{ V}$ and 100 V , respectively (the CEO refers to the base being left as an open circuit) [13-14]. However, these are minimum breakdown voltages, as shown in the figure above. Since a requirement for this laser driver is its ability to deliver pulses on a trigger, the base will not be left open and the actual breakdown voltages will be higher. This makes it necessary to have a high voltage power supply to achieve avalanche breakdown. The following subsection presents the schematic for the avalanche driver.

3.1.1 Avalanche Driver Schematic

The avalanche driver relies on a capacitor that is charged by a high voltage power supply. This capacitor acts as the current source once a trigger signal is received and the transistor enters the avalanche region. The capacitor discharges through the transistor and the laser diode to provide the necessary pulse [15]. The schematic for our avalanche driver is shown below.

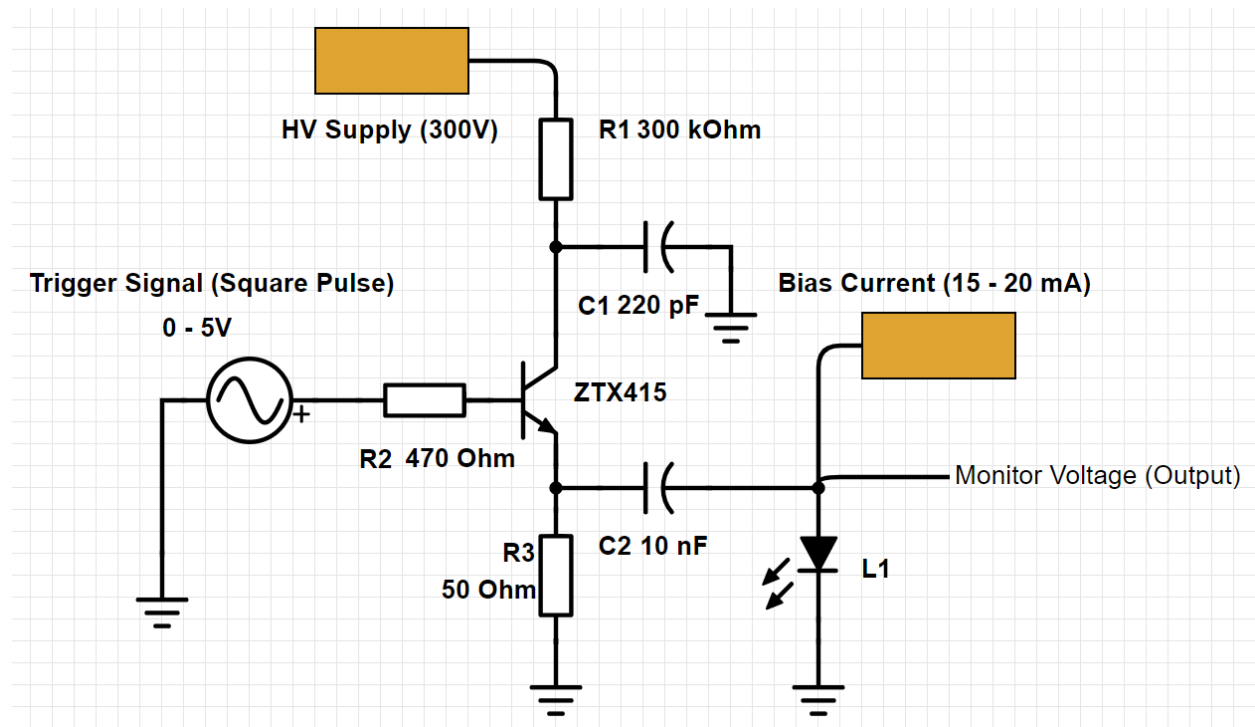


Fig 5: Avalanche laser driver design [adapted from 15]

The driver is triggered by a 0 - 5V pulse from the controller. While the transistor base is held at 0 V, capacitor C1 is charged from the high voltage (HV) power supply. As shown in figure 3 in the previous section, the highest breakdown voltage occurs when the base is grounded. As long as the HV supply voltage is below this value, the transistor will not avalanche. However, when the trigger is applied, the avalanche switches on and avalanches to deliver a large peak current and

short pulse by discharging C1. The pulse width (t_p) and peak current (I_p) can be controlled by the capacitor C1. These parameters can be related to the capacitance (C_1) and the supply voltage (V_s) with the following approximation:

$$C_1 V_s = t_p I_p \quad \text{eq (2)}$$

Although the avalanche-based laser driver can deliver narrow, high power pulses, it has two shortcomings:

- A high voltage power supply must be present in the final LIDAR system
- The rise time of the trigger signal pulses must be very low (less than a nanosecond), so that we have an accurate estimate of when the pulse is delivered to the laser diode. This will allow more accurate sampling using techniques such as equivalent time sampling (ETS) when a fast sampling system is not available.

These shortcomings can be resolved with a MOSFET based laser driver that is described in section 3.2.

3.1.2. Pulse and Parasitic Modelling

The short pulses in the laser driver make it necessary to model the electrical pulses in order to see the effect of parasitic components. The principal concern for parasitic effects in the avalanche driver is the C2 coupling capacitor that connects to the laser diode and isolates any DC signal coming from the transistor. The capacitor must be selected so that the pulse to the laser diode is not significantly distorted or attenuated. This coupling capacitor is equally important in the

switching driver that will be mentioned in the next section. In that case the capacitor acts to isolate the DC signal from the monitor signal in the driver so that only the high frequency components pass through. This allows us to model the capacitor as a high pass filter. In a typical RC high pass filter shown below, the 3 dB cutoff frequency is given by $f_c = \frac{1}{2\pi RC}$.

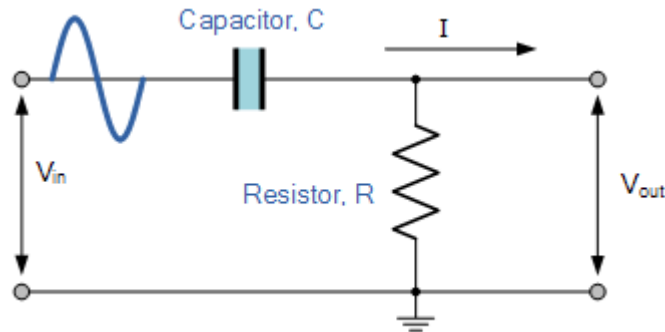


Fig 6: Passive RC high pass filter [16]

However, the parasitic inductance in the capacitor forces the capacitor to have a frequency cutoff known as the Self Resonant Point (SRP). With an ideal capacitor, the impedance ($Z_c = \frac{1}{j\omega C}$) decreases as the frequency is increased, and this is ideally what we want so that the high frequency components are coupled to the output. However, the parasitic inductor (with impedance $Z_L = j\omega L$) begins to contribute significantly to the impedance beyond the SRP point. This causes the impedance to increase at higher frequencies [17]. A graph of the impedance in surface mount capacitors is shown below and it illustrates the problems with using higher value capacitances. The graph shows that the SRP (indicated by the sharp fall and rise in impedance) occurs at lower frequencies for high capacitances.

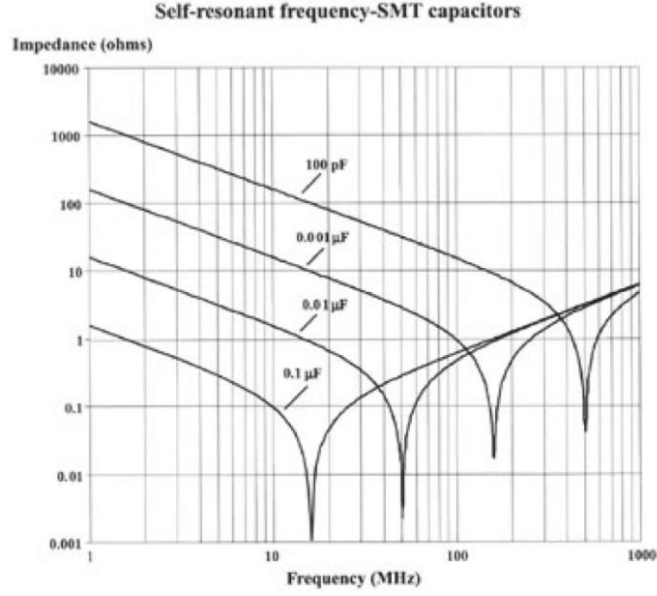


Fig 7: Figure showing Self resonant frequency of capacitors [17]

The coupling capacitor was modelled with its parasitic resistance and inductance and a Gaussian pulse with a full-width-half-max (FWHM) of 5 ns (which was observed during prototyping) was delivered through these components. The FWHM is used as an indicator for the pulse width. The values for the parasitic inductance used in this model were obtained from K-Sim [18]. The Gaussian pulse can be modelled with the following function

$$V(t) = ae^{-\frac{(t-b)^2}{2c^2}} \quad \text{eq (3)}$$

where a, b, c are constants that determine the pulse maximum, offset, and scaling (width), respectively. A 5ns FWHM gives

$$FWHM = 5 \text{ ns} = 2.35 c \rightarrow c = 2.1 \text{ ns}$$

The following figure shows the voltage source responsible for generating the pulse (B1) and parasitic components (R1, L1) that are modelled as part of the capacitor C1.

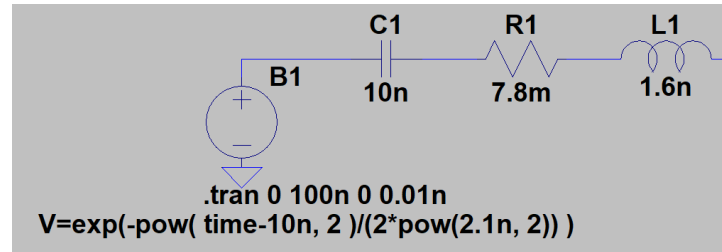


Fig 8: Modelling parasitic components of capacitor

A figure of the 5 ns Gaussian pulse is shown in the figure below, along with a Fourier transform of this signal. The Fourier transform shows that although the pulse is narrow with sharp rise times, a 100 MHz analog receiver should be able to record it without significant distortion. It is a different story to sample the signal to achieve a good waveform representation of the signal and this depends on the sampling rate of the system. The Rohde & Schwartz – RTM 2034 oscilloscope had a sufficiently fast sampler for prototyping.

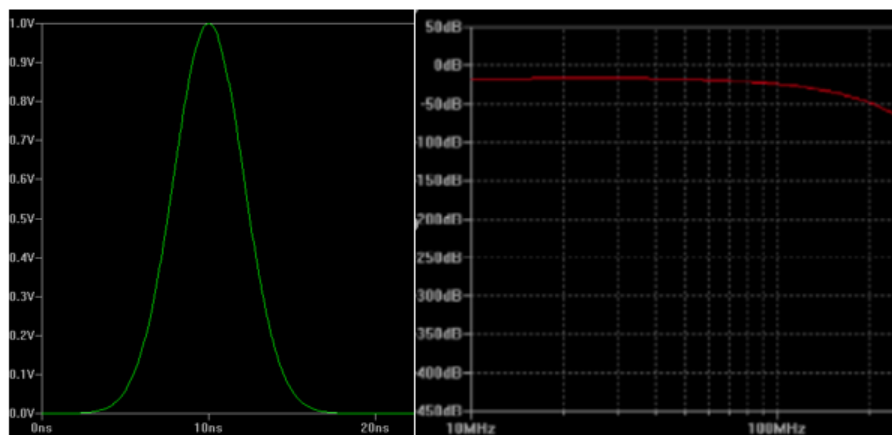


Fig 9: Left - Time domain model of an avalanche pulse with 5ns FWHM. Right – Frequency spectrum of avalanche pulse

The simulation from LTSpice using the Gaussian pulse and the parasitic components showed that a 10 nF coupling capacitor is suitable and does not distort our signal significantly.

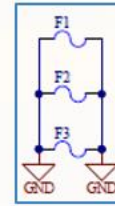
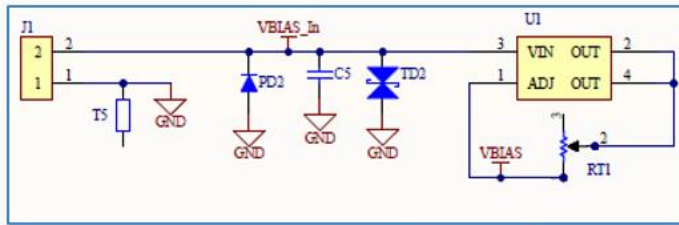
3.1.3 EMI Shielding

The short pulses described in the previous section can lead to Electromagnetic Interference (EMI) if these pulses travel through long traces or wires. This was found to be a problem when prototyping on a breadboard and delivering the laser pulse to the diode through wires. The EM noise pose significant problems if they fall onto a wideband receiver as they can mask out the received optical signal. The solution to minimize EMI noise in this project was to use a grounded faraday cage to contain the noise emitted from the driver circuit. The trace lengths for the circuitry near the transistor were kept to a minimum to ensure the emitted noise was minimized.

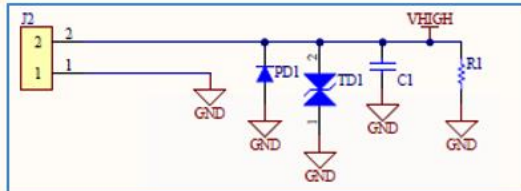
3.1.4 Avalanche Driver Implementation

The final implementation for the avalanche driver circuit is shown in the following figure.

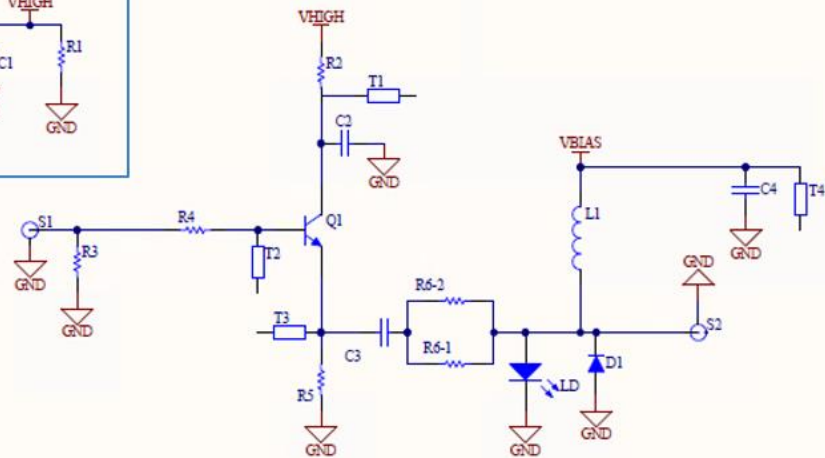
Bias input branch



EMI Shielding



High Voltage input branch



Avalanche driver circuit

Fig 10: Schematic for avalanche driver circuit

The following list describes the various stages shown in the schematic:

- The bias input branch contains an LM317 chip in a constant current source configuration (adjustable with the RT1 potentiometer) to provide the bias current to the laser diode. The bias current is important for laser diodes because of their *threshold current* parameter. The threshold current specifies the minimum current required to achieve lasing so that the laser diode provides coherent light through stimulated emission (instead of spontaneous emission). During lasing, the diode also provides higher optical power when the current increases, similar to the forward voltage in a diode. The

bandwidth in nanometers becomes narrower, so that a laser diode rated at 650 nm does not have many spectral components away from 650 nm [19].

- The EMI shield branch consists of holders for a faraday cage that are connected to ground. These are present to minimize noise due to EMI, as described in the previous section.
- The high voltage input branch contains a decoupling capacitor to minimize noise in the DC signal that is reaching the avalanche driver. A high value resistor ($300\text{ k}\Omega$) is connected to ground to ensure the capacitor C2 discharges sufficiently quickly when the high voltage power supply is disconnected.
- The avalanche driver circuit is described in section 3.1.1. Figure 9 shows two SMA connectors (S1, S2) that are used to receive a trigger pulse and provide an output monitor waveform. This is an important specification for the driver. The test points (T1, T2, T3, T4, T5) allow the user to use an oscilloscope to measure the signals at these nodes. The coupling capacitor described in section 3.1.2 is shown as C3 (10 nF), and this is connected to resistors R6-1 (a bypass $0\text{ }\Omega$ resistor) or R6-2 ($22\text{ }\Omega$). These two resistors provide flexibility with how the laser diode is connected to the transistor and only one will be used at a time. The inductor L1 acts as a high frequency choke so that the laser pulse does not travel to the bias circuitry. Finally, the diode D1 acts as a reverse polarity protection for the laser diode (LD).
- The driver uses regular diodes (PD1, PD2) and Transient-voltage-suppression (TVS) (TD1, TD2) to protect the board from accidental reverse polarity connections and from unacceptable transient voltages. The TVS diodes were selected so that they were rated slightly above the maximum input voltage the driver was designed for.

The 3D model for the PCB designed from this schematic is shown in the following figure. This driver's performance is discussed in the results section.

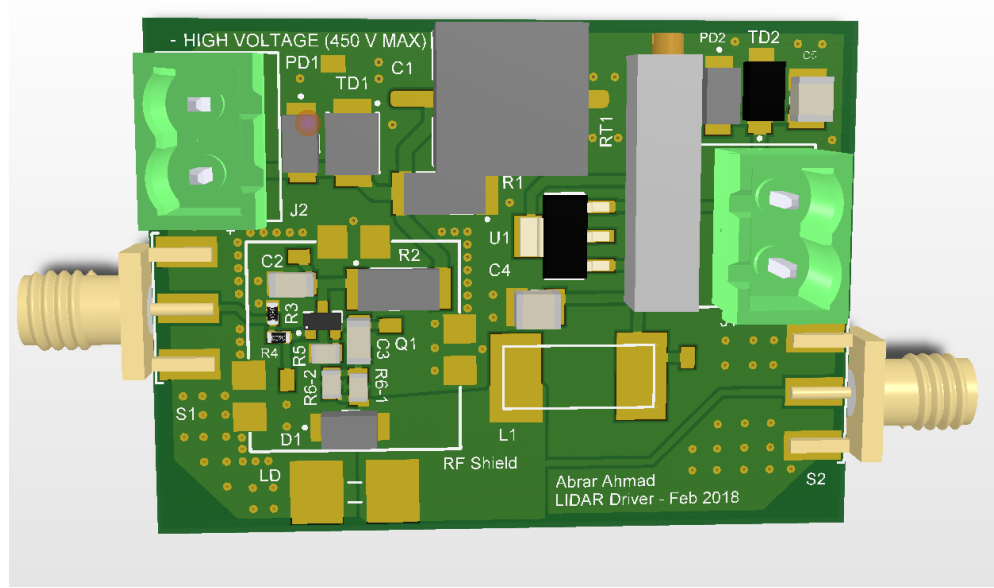


Fig 11: PCB for avalanche driver

3.2 Laser Driver II: MOSFET Switching

3.2.1 Switching Driver Schematic

The avalanche driver allows short pulses with high peak currents to be delivered. A MOSFET can be replace the transistor, as long as the MOSFET has a low turn-on resistance ($R_{DS(ON)}$). This driver operates by charging a capacitor bank and discharging it through the laser diode as the MOSFET turns on. If $R_{DS(ON)}$ is low, the current delivered through the laser diode will be high.

A MOSFET driver is used to provide rapid switching for the MOSFET. This driver allows the charge on the gate of the MOSFET to be transferred and removed quickly so that short rise and fall times are achieved. The short rise/fall times will ensure that the pulse width can be kept small. The avalanche driver is able to generate short pulses on its own. Although the switching driver is able to provide large peak currents, it requires an input pulse that can ensure that the MOSFET is kept on for a short time (on the order of nanoseconds, which is the pulse width we want from our driver). This requirement was satisfied by placing a pulse generator on the driver PCB. The functionality discussed above is summarized in the following figure.

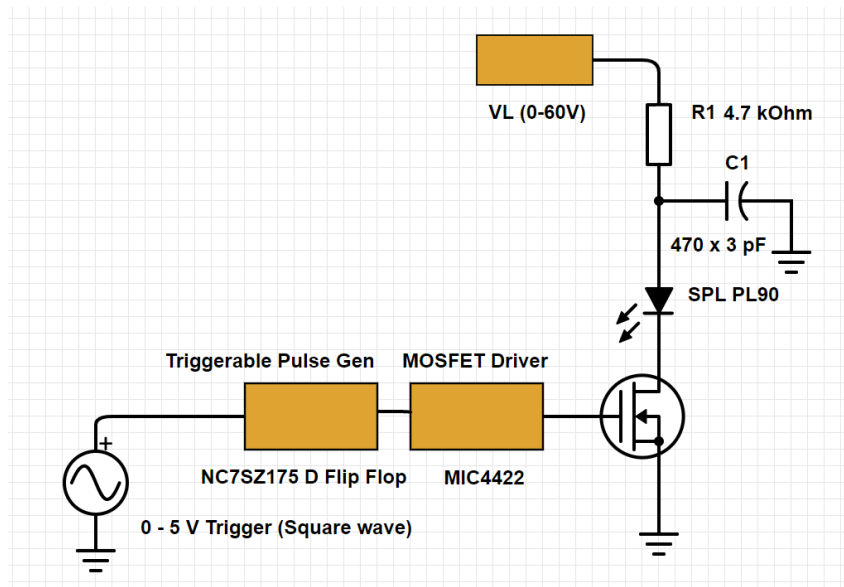


Fig 12: MOSFET based laser driver [adapted from 20]

The onboard pulse generator is made with an asynchronous D flip flop and relies on the propagation delay between the trigger input and the reset terminal of the flip flop, which are connected through a resistor. The design is shown in the following schematic.

The trigger allows the output of the flip flop to go “high” This allows the trigger input’s pulse width to be arbitrarily long, as long as the rise time is short. The following figure shows the pulse generator using an asynchronous D flip flop. A simple pulse generator is created that uses the delay in resetting an asynchronous D flip flop right after the clock latches the output HIGH, as shown in the schematic below.

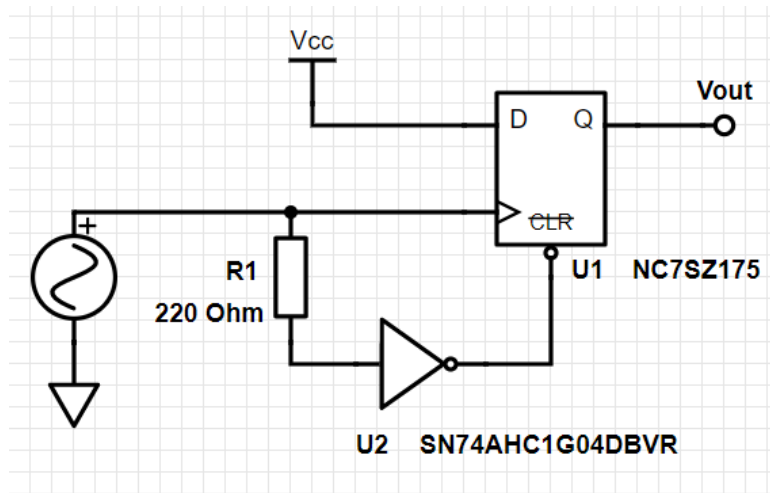


Fig 13: Pulse generator based on propagation delay between input and CLR terminal

Once the trigger signal goes “high” the output will follow and become “high”. The trigger signal will propagate through the resistor and inverter and will arrive at the reset terminal after it has already reached the clock input of the flip flop. As long as propagation delay of the reset path is longer than the time it takes for the flip flop to latch the “high” output, the pulse generator is able to generate pulses less than 100 ns wide. The pulse width can be controlled by the resistor (a higher resistance will increase the pulse width). The inverter is required because most flip flops available have an inverted CLR input. This does not pose a problem as long as the propagation

delay of the inverter is not too high. The inverter selected above has a maximum propagation delay of 4.5 ns at 5 V from the datasheet [21].

3.2.2 Switching Driver Implementation

The final implementation for the switching driver circuit is shown in the following figure.

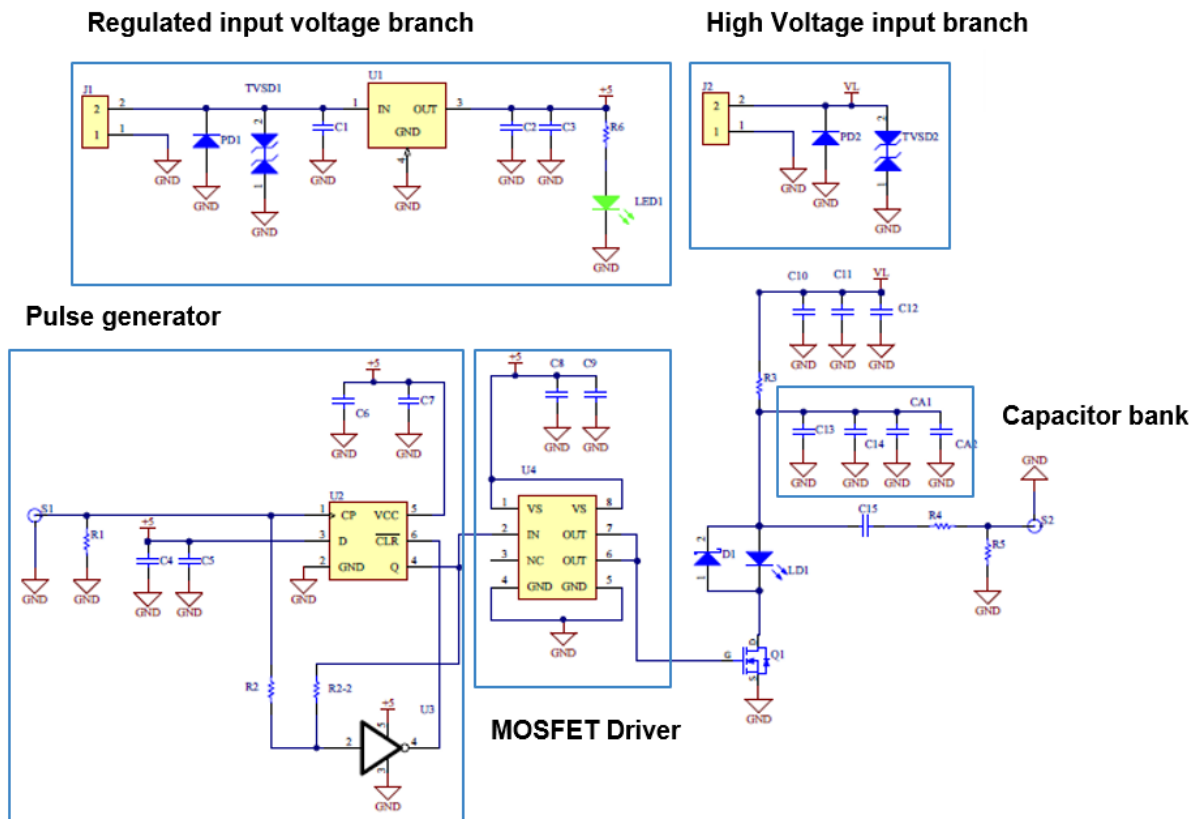


Figure: Schematic for switching driver

Fig 14: Schematic for switching driver circuit [adapted from 20]

The following list describes the various stages shown in the schematic:

- The Regulated bias input branch provides a 5 V input voltage to power the flip flop (U2), inverter (U3) and MOSFET driver (U4) using a fixed 5 V regulator (U1). As recommended by the datasheet, two decoupling capacitors are placed on the regulator's output [22]. An indicator LED is placed after the regulator so that the user can easily see when the circuit is plugged in.
- The capacitor bank contains four 470 pF capacitors to allow a large amount of charge to be discharged through the laser diode when the MOSFET (Q1) is switched on. Q1 has a low turn on resistance ($27\text{ m}\Omega$) to provide a low-resistance path and maximize the current through the laser diode. The capacitor bank is connected to the high voltage input branch with 3 decoupling capacitors (C10 – C12) to remove any noise coming from the high voltage source.
- As with the avalanche driver, two SMA connectors (S1, S2) that are used to receive a trigger pulse and provide an output monitor waveform.
- An optional resistor (R2-2) is connected to the flip flop's output (U2). This can replace the R2 resistor if the pulse generator described in the previous section does not work because the propagation delay of the (R2, U3) path is shorter than the time it takes for the flip flop to output "high".
- The MOSFET driver (U4) is connected directly to the MOSFET (Q1) to allow for short rise/fall times. These components are placed close to each other on the PCB to minimize transit times in the traces.

- The diode D1 acts as a reverse polarity protection for the laser diode (LD). The diodes PD1, PD2 protect the overall circuit from reverse polarity, while the TVS diodes (TVSD1, TVSD2) offer protection from transient spikes.

The 3D model for the PCB designed from this schematic is shown in the following figure. This driver's performance is discussed in the results section.

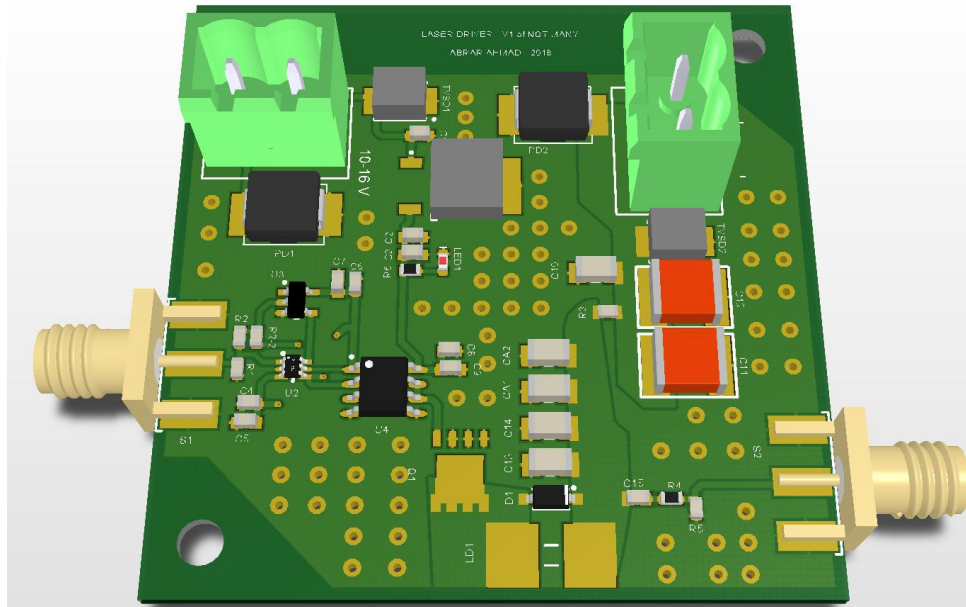


Fig 15: PCB for switching driver

3.3 Optics Assembly

The LIDAR is intended to operate at large distance (up to 20 m). In order to achieve this, a collimated laser beam is required so that the optical power does not disperse before it reaches the obstacle. The transmitter assembly uses an aspheric lens (A390TM-B) to collimate the beam. The lens is mounted inside a small 1.5" tube from Thorlabs (S05TM09) to minimize the footprint

of the overall transmitter. A laser diode mount (S05LM46) with threads that match the tube is used to put the laser diode inside the tube firmly. The aspheric lens has a broadband (wavelength) anti-reflection coating to allow us to switch laser diodes in the future. The following figure shows the reflectance graph of the coating that was selected.

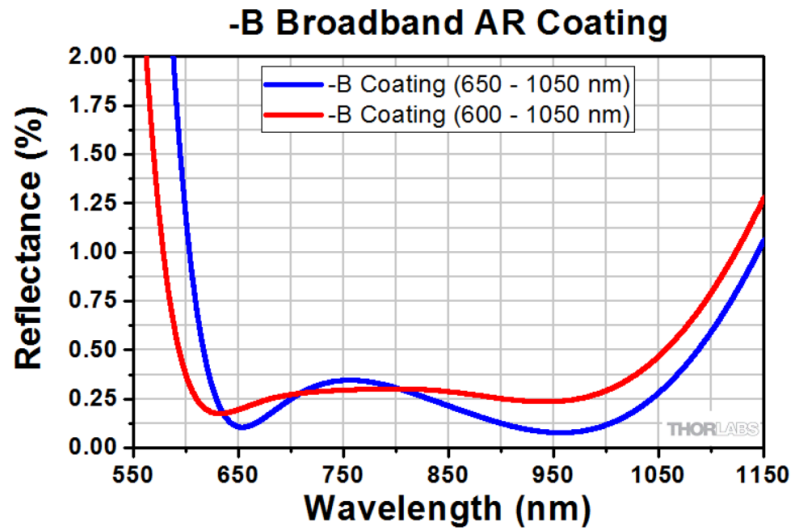


Fig 16: Reflectance graph for the coating selected for the asphere lens [23]

The following figure shows the principle of collimation with an aspheric lens.

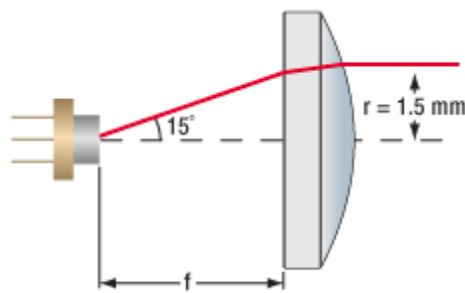


Fig 17: Illustration of beam collimation with aspheric lens [24]

The maximum beam divergence for the L650P007 is 24° from the datasheet [8]. The A390TM-B Aspheric lens from Thorlabs has a focal length of $f = 4.6 \text{ mm}$ [23]. This gives a collimated beam radius as [24]

$$r = 4.6 \text{ mm} \times \tan\left(\left(\frac{24}{2}\right)^\circ\right) = 0.98 \text{ mm}$$

The tube assembly is shown along with the PCBs in section 4.1.

3.4 3D Printing Mechanical Assembly

Although the laser diode is mounted to the tube with a special mount (described in the previous section), it is necessary to have a rigid support connecting the leads of the laser diode to the PCB. This is important because the laser diode is only supported by solder at its pins. A holder was designed and 3D printed to overcome this problem. The dimensions of the laser driver PCB were measured and the design was made with the Fusion 360 software. The *Ultimaker 2* 3D printer at the uOttawa Richard L'Abbe Makerspace was used to print the assembly. The figure below shows the holder's design.

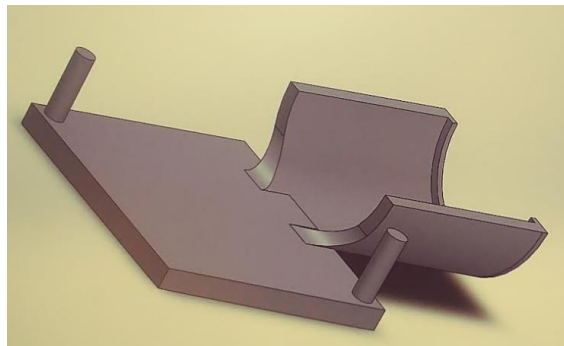


Fig 188: CAD model for driver holder

The 3D printed holder is discussed in the results section.

4 Achievements

The results of this project are discussed here. The performance of the two drivers that were made is presented. The implemented optics and holder assemblies that were outlined in the previous section are described. An alternative design for the laser driver is also presented here.

4.1 Results

4.1.1 Avalanche driver

4.1.1.1 Transistor Selection and EMI

The avalanche laser driver was prototyped on a breadboard and tested with two transistors to select a transistor for the PCB: 2N2369A and ZTX415. The output pulses of the two transistors were recorded for various discharge capacitors (see section 3.1.1). The following figure shows two traces with the 2N2369A transistor. The yellow trace shows the voltage across a 90pF discharge capacitor while the green trace shows the voltage across the laser diode. It can be seen from the figure that the capacitor is charged to approximately 130V while the transistor base input is held at 0 V. The base is then triggered to 5 V and the voltage across the capacitor rapidly decreases. Simultaneously, it can be seen that the voltage across the laser diode rises to approximately 60 V.



Fig 19: Trigger and avalanche pulse signals using 2N2369A transistor

The 2N2369A was replaced with the ZTX415 transistor, which is specified as an avalanche transistor in the manufacturer datasheet [14]. A snapshot of the traces with this transistor was taken. A 90 pF discharge capacitor was used and the traces across the capacitor (green) and the laser diode (yellow) are shown in the figure below. This figure shows that the capacitor charges to 380 V. The peak avalanche pulse voltage is seen to be 180 V with a pulse width FWHM as approximately 5 ns.



Fig 20: Trigger and avalanche pulse signals using ZTX415 transistor

Although the driver can provide high peak powers at short pulses to the laser diode, it cannot be tested successfully at this stage. This is due to the EMI noise (described in section 3.1.3) that is generated as the transistor avalanches (on the breadboard implementation). The EMI signal was detected by using one of the oscilloscope probes as an antenna. The figure below shows that a transistor delivering pulses with a peak voltage of 100 V generates a $10 V_{peak-to-peak}$ EMI signal.

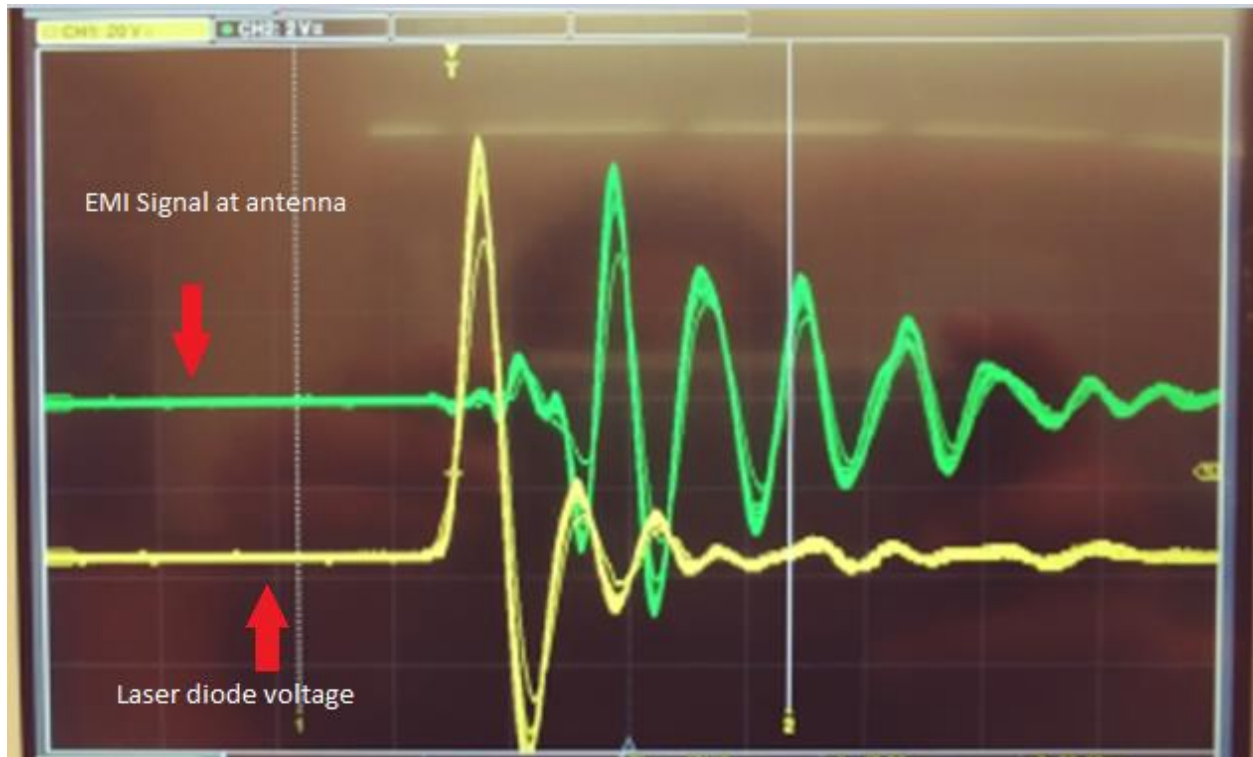


Fig 21: Avalanche and noise signals from driver using ZTX415 transistor

This prevents accurate measurement of the optical pulse unless the receiver circuit or laser driver circuit are properly shielded from EMI. This is combatted with a faraday cage and short traces, as discussed in section 3.1.3. The PCB development led to the conclusion that a MOSFET driver is a good alternative and should be built developed simultaneously. This driver is described in the next section.

4.1.1.2 PCB Implementation

The PCB outlined in section 3.1.4 was manufactured from ALLPCB in China and a reflow oven was used to solder surface mount components. A stencil was ordered along with the PCB and solder paste was used to mount these components. The final board is shown in the figure below.

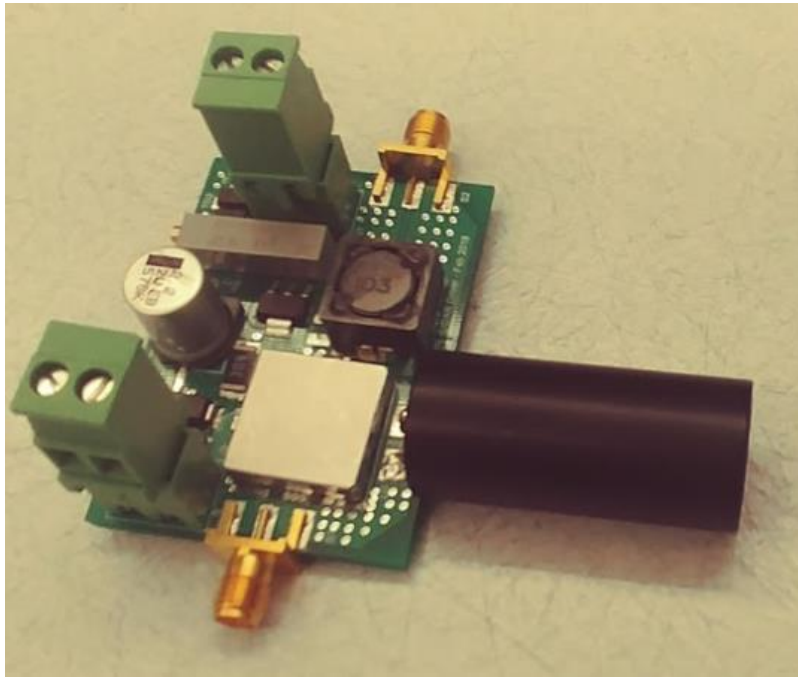


Fig 22: Implementation of avalanche driver

The transistor, discharge capacitor, decoupling capacitor and most of the circuitry involved in biasing the transistor are placed under the grounded Faraday cage (shown in silver above) to minimize EMI. The laser diode is placed inside the tube with a laser diode mount. The 3D printed holder is described alongside the switching driver in the next section.

This PCB worked successfully and is capable of delivering 10 nanosecond pulses with high peak voltages to the laser diode. The following figure shows the results from this driver.



Fig 23: Measured traces from avalanche driver PCB

The figure above shows that a high voltage pulse is delivered when the trigger goes high (5 V). The high voltage trace was obtained from the SMA monitor output of the driver and the trigger was delivered through the SMA input. This satisfies the specifications for the laser driver.

4.1.2 Switching driver

4.1.2.1 Testing MIC4422 MOSFET driver for switching

The switching driver requires a MOSFET driver to rapidly turn the MOSFET on and off. It was therefore crucial to select a driver that provides low rise/fall times. The MIC4422YN driver was

tested with the HUF76423P3 MOSFET from Fairchild Semiconductor. The figure below shows the test circuit for the MOSFET driver. When the MOSFET turns on, the test point will be grounded.

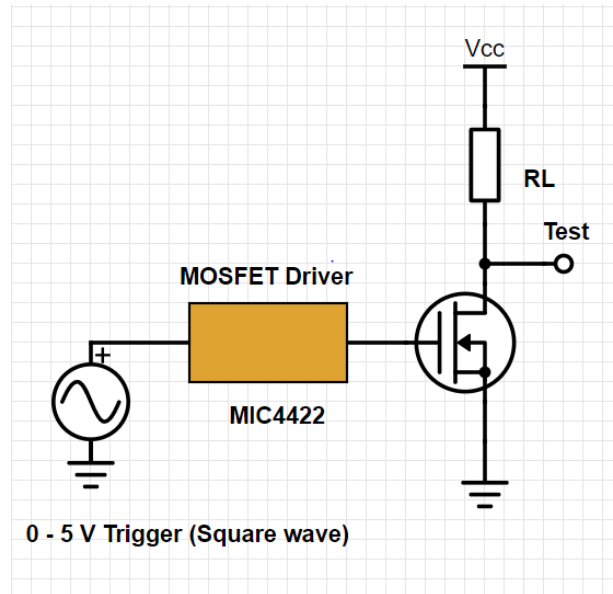


Fig 24: Test circuit for MOSFET driver

The figure below shows a trace for the trigger input (green) and the output signal (yellow). We see that the turn on time (falling edge of the yellow trace) is about 20 ns.



Fig 25: MOSFET switching with MIC4422YN driver. Green trace: Trigger input to driver. Yellow trace: voltage at output

The table below summarizes the turn on and off times with and without the driver.

	Turn on time [ns]	Turn off time [ns]
With MOSFET driver	20	2000
Without MOSFET driver	50	2500

Table 1: Turn on/off times with and without the MIC4422 driver

The table shows that the MOSFET driver provides faster turn on and turn off. The turn off time with the driver is very high ($2 \mu\text{s}$) and this is unexpected. A possible reason for this is that the testing was performed on a breadboard and where the driver and MOSFET are placed at a large distance. We expect the MOSFET to turn off faster when it is put onto a PCB and the two ICs are placed close together on the board.

4.1.2.2 PCB Implementation

The PCB outlined in section 3.2.2 was manufactured from ALLPCB and soldered in the reflow oven, like the avalanche driver. The final board is shown in the figure below.

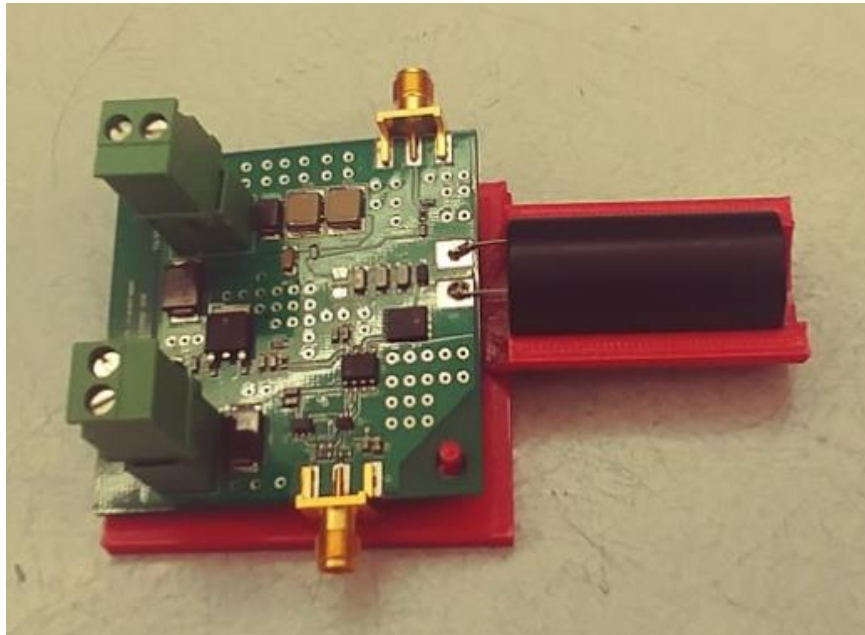


Fig 26: Implementation of switching driver

This driver was difficult to solder due to the small size of the inverter used in the pulse generator (described in section 3.2.1). The LED in this turned on and indicated that the input branch of the circuit was working properly. However, this driver could not generate pulses. The board was tested extensively, at all the inputs and the pins of the flip flop, inverter and driver ICs. It was found that the trigger signal did not reach the pulse generator and so the flip flop never latched to the input to provide a “high” output. Since the avalanche circuit worked and satisfied the specifications for the laser driver in the LIDAR system, another PCB was not developed for the switching driver.

4.2 Alternative Designs

This section lists two alternative designs for the laser driver. One of these designs (the switching driver) was implemented unsuccessfully in this project and can be redeveloped to work properly. A different design for the switching driver is proposed, as well as a third design for the laser driver that utilizes a coaxial cable to generate pulses.

4.2.1 (Successful) Switching laser driver with Alternative Pulse Generator

The switching laser driver that was described in section 3.2 was manufactured and tested, but it did not work as expected. The pulse generator with the asynchronous D flip flop was found to be the problem. An alternative pulse generator that does not rely on propagation delays in the flip flop is proposed here. The following figure shows a nanosecond pulse generator from Analog Devices [25].

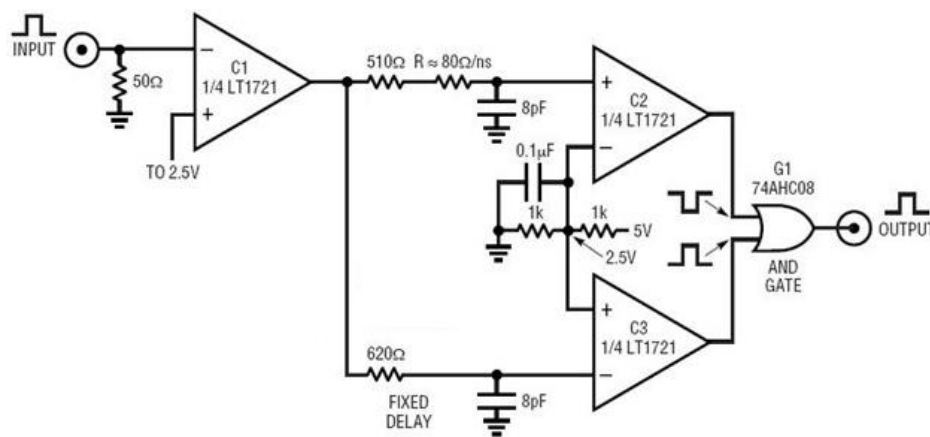


Fig 27: Pulse generator using comparators with an AND gate [25]

This pulse generator has a resistor that provides a fixed propagation delay to one comparator (C3 in the figure above) and another resistor + comparator branch (C2) is used to provide a variable delay. The fixed delay resistor is connected to the negative terminal of the comparator, while the variable delay is connected to the positive terminal. This ensures that the output from C2 goes “low” when the pulse reaches the comparator, and the output from C3 goes “high” when the pulse is received. Since the resistance on the C2 path is smaller than the resistance on the C3 path, the output of C2 will go “high” before the output of C3 goes “low”. The output from the AND gate will be high during this time (as long as the gate propagation delay is small). According to Analog Devices, the variable delay branch in figure 28 provides 1 ns for every 80 Ω of resistance. This pulse generator has successfully been used in the EPC9126 commercial laser driver [20].

The switching laser driver is a good alternative to the avalanche driver because it provides two significant advantages:

1. The input voltages required for the switching driver are much lower than the avalanche driver, which was found to require over 230 V.
2. The switching driver provides the ability to change the pulse width if the pulse generator described above is used with a variable resistor. This is not easy to achieve in the avalanche driver because the transistor discharges the capacitors rapidly during avalanching.

4.2.2 Rangefinder with Step Recovery Diode (SRD) and Coaxial cable

An alternative design using a shorted coaxial cable with a step recovery diode (SRD) is capable of providing pulses with widths less than 1 nanosecond and allows the repetition rate to be brought up to 80 MHz [26]. This repetition rate is difficult to achieve with the avalanche driver unless the high voltage (HV) power supply is capable of providing more power. The current HV supply uses a boost converter topology and this cannot maintain a high voltage if the current draw from the supply is high. The main issue is with the power supply's ability to maintain the charge on the output capacitor. The power supply in this project could not be used to provide repetition rates greater than 20 kHz. The following figure shows the SRD + coaxial cable based laser driver from a publication [26].

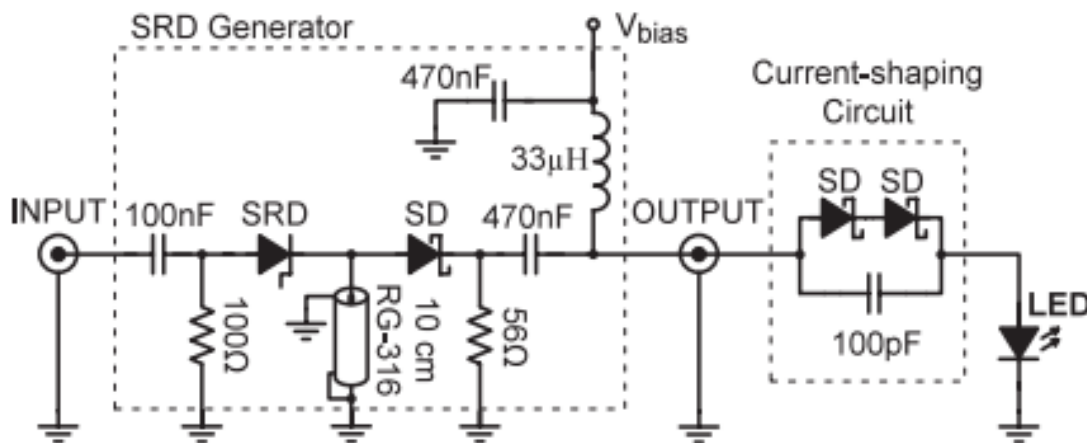


Fig 28: Laser driver based on SRD and coaxial cable [26]

The SRD in the figure is capable of providing negative pulses, but these pulses do not allow the Schottky diode (SD before the OUTPUT) to conduct. The pulse travels through the shorted coaxial cable and is reflected back once it reaches the end [26]. This polarity of the reflected pulse

changes and the Schottkey diode is able to conduct. This is prevented from travelling through the bias branch by the choke inductor and travels to the laser diode. One major advantage of this design is that no avalanche transistors and MOSFET drivers are required to achieve low rise/fall times. The pulse width depends on the length of the waveguide, which is a coaxial cable in this case.

4.3 Discussion

The high speed laser driver developed in this laser driver is discussed extensively in the results section (4.1). The results showed that the avalanche driver met the specifications of the laser driver by providing the following capabilities:

1. A trigger pulse could be provided through an SMA connector
2. A monitor output could be obtained through an SMA connector to determine the electrical pulse that is delivered to the laser diode
3. Nanosecond pulses with 10 nanosecond pulse widths could be delivered to the laser diode
4. The peak voltage for the electrical pulses was high (150 V)

It is also desirable to have a high repetition rate for the pulses so that the number of pulses that are delivered per unit time is maximized. This repetition rate is found to depend on the power supply that is available and can be increased if the power supply is capable of maintaining a high

voltage while the avalanche transistor is triggered at a higher repetition rate (as long as the capacitor is able to charge to the required breakdown voltage).

Another accomplishment for the avalanche driver is the small footprint. The final PCB was less than 6 cm long and 4 cm wide. This will allow the final LIDAR system to be contained in a small enclosure to allow for better portability. Since the driver was designed successfully, a two-sided PCB can be used to dramatically decrease the footprint. An appropriate way of doing this is to place all the components that are enclosed in the faraday cage on one side and the remaining circuitry on another side of the PCB. This will also allow the trace connected to the output SMA connector to be shortened. This trace is the longest trace on the board and it is suspected that this contributes to EMI noise.

Since there was no optical receiver available when the laser driver was completely tested, there was no way to monitor the optical pulses delivered by the laser driver. The electrical pulses were characterized but it is possible for issues to arise in the optical pulse. To compensate for this and to ensure that the laser driver was providing pulsed power, a rudimentary check was performed. Since a higher repetition rate corresponds to a higher average power delivered to the laser diode, the repetition rate was increased to the power supply's capabilities and the optical power of the laser diode was seen to increase, by observing the laser diode getting brighter.

The advantages of the switching driver were outlined in sections 3.2 and 4.2.1. The switching driver was developed as an alternative design to the avalanche driver because it would reduce the power requirements from the high voltage power supply. The current design of the switching driver is capable of satisfying the specifications outlined in section 1.3, but further work needs to be done to ensure that the on-board pulse generator works properly.

5 Conclusion

5.1 Summary

A pulsed laser driver was developed for a LIDAR sensor in this project. As discussed in this report, LIDAR sensors have gained prominence in the autonomous car industry. This has led a number of companies (e.g. Quanergy) to promise cheap LIDAR sensors that can be integrated into autonomous car solutions. However, harsh weather conditions pose a challenge for LIDAR sensors because they attenuate the optical signal. The laser driver developed in this project is capable of providing high peak powers so that the signal attenuation from atmospheric particles is not crippling. The driver is capable of providing short pulse width to increase the spatial resolution of objects. A number of alternative designs for the pulse generators and laser drivers were given in this report to allow the pulse widths to be increased. This may be beneficial in systems that do not have a fast sampler or a high bandwidth for the receiver.

5.2 Contributions

The main contribution of this project is laser driver for the LIDAR sensor. This driver was developed as a standalone driver and it is not tied to the LIDAR sensor. This approach offers a major advantage because the laser driver can be used in a number of alternative applications. A list of these is included below:

- The laser driver can be used to characterize fog or other atmospheric conditions as part of research studies.
- The collimation lens used with this laser driver has a wideband anti-reflection coating (as mentioned in section 3.3). This provides a degree of flexibility because an infrared laser diode can be used with the driver without making any changes in the design. This allows the ability to determine signal attenuation as a function of wavelength in particular harsh weather conditions.
- The laser driver is compact and easily transportable. The SMA connectors allow the user to conveniently supply and receive signals from the driver using portable function generators or sampling hardware.

5.5 Future Work

Although the laser driver was capable of delivering electrical pulses according to the specifications outlined in section 1.3, it is important to characterize the optical pulses. An optical receiver with a minimum bandwidth of 100 MHz (determined in section 3.1.2) is required in order to measure the pulse accurately. The receiver designed as part of the LIDAR project was not

working at the time this driver was made and it is important to characterize the optical pulses with a functional receiver.

The laser driver was developed with a 650 nm laser diode (L650P007 from Thorlabs), but an infrared laser diode (SPL PL90 from OSRAM) was also purchased. This laser diode is rated as a pulsed laser diode, and it would be beneficial to test the driver with this. The performance of these lasers can be compared in the fog.

Since the switching laser driver has been designed and implemented on a PCB, this should be debugged further to find the solution. A duplicate set of parts is available to implement this driver again and confirm whether the connections and/or components are the problem.

6 References

- [1] R. Amadeo, "Google's Waymo invests in LIDAR technology, cuts costs by 90 percent", 2017. [Online]. URL: <https://arstechnica.com/cars/2017/01/googles-waymo-invests-in-lidar-technology-cuts-costs-by-90-percent/>. [Accessed 10-Apr-2018].
- [2] C. McGoorgan, "Google is testing how driverless cars work in the rain", 2016. [Online]. URL: <https://www.telegraph.co.uk/technology/2016/02/04/google-is-testing-how-driverless-cars-work-in-the-rain/>. [Accessed 10-Apr-2018].
- [3] E. Ackerman, "Quanergy Announces \ \$250 Solid-State LIDAR for Cars, Robots, and More", 2016. [Online]. URL: <http://spectrum.ieee.org/cars-that-think/transportation/sensors/quanergy-solid-state-lidar>. [Accessed 10-Apr-2018].
- [4] J. Guo, "Propagating Characteristics of Pulsed Laser in Rain", International Journal of Antennas and Propagation, 292905, 2015.
- [5] A. Filgueira et al., "Quantifying influence of rain in LIDAR performance", Science Direct, 95, 2017.
- [6] A. Vydhyathan, "Effect of Atmospheric Particulates on Airborne Laser Scanning for Terrain-referenced Navigation", 2000. [Online]. URL: https://etd.ohiolink.edu/!etd.send_file?accession=ohiou1163793662&disposition=inline. [Accessed: [Accessed 10-Apr-2018].
- [7] C. Wolff, "Range Resolution". [Online]. URL: <http://www.radartutorial.eu/01.basics/Range%20Resolution.en.html>. [Accessed 10-Apr-2018].

- [8] Thorlabs, "Product Specification Sheet – L650P007". [Online]. URL: <https://www.thorlabs.com/drawings/b09a2f23923b3638-2B6EE000-E36F-331D-9818D680D531A036/L650P007-SpecSheet.pdf>. [Accessed 11-Apr-2018].
- [9] Laser Safety Facts, "Class 3B (IIIb) laser safety information". [Online]. URL: <http://www.lasersafetyfacts.com/3B/>. [Accessed 11-Apr-2018].
- [10] Professional Engineers Ontario, "About PEO". [Online]. URL: http://www.peo.on.ca/index.php?ci_id=1812&la_id=1. [Accessed 11-Apr-2018].
- [11] S. McGarry, "ELEC 3908 – Physical Electronics Courses Pack Fall/Winter", 2014. [Online]. cuLearn, DoE. [Accessed 11-Apr-2018].
- [12] B. W. Williams, "Power Electronics: Devices, Drivers, Applications, and Passive Components", McGraw-Hill, 1992.
- [13] Central Semiconductor Corp., "2N2369A – Silicon NPN Transistor", 2014. [Online]. URL: https://www.centralsemi.com/get_document.php?cmp=1&mergetype=pd&mergepath=pd&pdf_id=2n2369a.PDF. [Accessed 11-Apr-2018].
- [14] Diodes Incorporated, "ZTX415 – NPN Silicon Planer Avalanche Transistor", 1995. [Online]. URL: <https://www.diodes.com/assets/Datasheets/ZTX415.pdf>. [Accessed 11-Apr-2018].
- [15] M. Gallant, "Speed of light with nanosecond pulsed 650nm diode laser", 2008. [Online]. URL: <https://www.elexp.com/Images/Speed of light with 650nm diode laser.pdf>. [Accessed 11-Apr-2018].

- [16] Electronics Tutorials, “Passive High Pass Filter”. [Online]. URL: http://www.electronics-tutorials.ws/filter/filter_3.html. [Accessed 11-Apr-2018].
- [17] Christian, “EMC re-validation driven by manufacturing plant or production changes”. [Online]. <http://www.flexautomotive.net/EMCFLEXBLOG/post/2015/07/10/emc-re-validation-following-manufacturing-plant-or-production-process-change>. [Accessed 11-Apr-2018].
- [18] K-Sim, “K-Sim – Ceramic”, 2017. [Online]. URL: <http://ksim.kemet.com/Ceramic/CeramicCapSelection.aspx>. [Accessed 11-Apr-2018].
- [19] W. Lee, “Lasers”, NCTU OpenCourseWare. [Online]. URL: <http://ocw.nctu.edu.tw/upload/classbfs120901572082809.pdf>. [Accessed 11-Apr-2018].
- [20] Efficient Power Conversion (EPC), “Development Board EPC9126”, 2017. [Online]. URL: http://epc-co.com/epc/Portals/0/epc/documents/guides/EPC9126_qsg.pdf. [Accessed 11-Apr-2018].
- [21] Texas Instruments, “SN74LVC1G04-EP Single Inverter Gate”, 2007. [Online]. URL: <http://www.ti.com/lit/ds/symlink/sn74lvc1g04-ep.pdf>. [Accessed 11-Apr-2018].
- [22] Diodes Incorporated, “AZ2940 1A Ultra Low Dropout Linear Regulator”, 2015. [Online]. URL: <https://www.diodes.com/assets/Datasheets/AZ2940.pdf>. [Accessed 11-Apr-2018].
- [23] Thorlabs, “Molded Glass Aspheric Lenses”. [Online]. URL: https://www.thorlabs.com/newgrouppage9.cfm?objectgroup_id=3811&pn=A390TM-B. [Accessed 11-Apr-2018].

[24] Thorlabs, “Choosing a collimation lens for your laser diode”. [Online]. URL:

<https://www.thorlabs.com/tutorials.cfm?tabID=f7ed0dd5-3f31-4f84-9843-e0f7ac33f413>.

[Accessed 11-Apr-2018].

[25] Analog Devices, “LT1721 Pulse Generator”. [Online]. URL:

<http://www.analog.com/en/design-center/reference-designs/circuit-collections/lt1721-pulse-generator-has-0ns-to-10ns-width-520ps-transitions.html#cc-overview>. [Accessed 11-Apr-2018].

[26] P. H. Binh et al., “A simple sub-nanosecond ultraviolet light pulse generator with high repetition rate and peak power”, Review of Scientific Instruments, 84, 083102, 2013.